Surg Today (2016) 46:214–223
DOI 10.1007/s00595-015-1160-0

ORIGINAL ARTICLE

Prediction of sentinel lymph node status using single-photon emission computed tomography (SPECT)/computed tomography (CT) imaging of breast cancer

Mai Tomiguchi[1] · Mutsuko Yamamoto-Ibusuki[1] · Yutaka Yamamoto[1,2] · Mamiko Fujisue[1] · Shinya Shiraishi[3] · Touko Inao[1] · Kei-ichi Murakami[1] · Yumi Honda[4] · Yasuyuki Yamashita[3] · Ken-ichi Iyama[4] · Hirotaka Iwase[1]

Received: 19 May 2014 / Accepted: 11 March 2015 / Published online: 19 April 2015

Abstract
Purpose Single-photon emission computed tomography (SPECT)/computed tomography (CT) improves the anatomical identification of sentinel lymph nodes (SNs). We aimed to evaluate the possibility of predicting the SN status using SPECT/CT.
Methods SN mapping using a SPECT/CT system was performed in 381 cases of clinically node-negative, operable invasive breast cancer. We evaluated and compared the values of SN mapping on SPECT/CT, the findings of other modalities and clinicopathological factors in predicting the SN status.
Results Patients with SNs located in the Level I area were evaluated. Of the 355 lesions (94.8 %) assessed, six cases (1.6 %) were not detected using any imaging method. According to the final histological diagnosis, 298 lesions (78.2 %) were node negative and 83 lesions (21.7 %) were node positive. The univariate analysis showed that SN status was significantly correlated with the number of SNs detected on SPECT/CT in the Level I area ($P = 0.0048$), total number of SNs detected on SPECT/CT ($P = 0.011$), findings of planar lymphoscintigraphy ($P = 0.011$) and findings of a handheld gamma probe during surgery ($P = 0.012$). According to the multivariate analysis, the detection of multiple SNs on SPECT/CT imaging helped to predict SN metastasis.
Conclusions The number of SNs located in the Level I area detected using the SPECT/CT system may be a predictive factor for SN metastasis.

Keywords Sentinel lymph node biopsy · Metastasis · SN mapping · SPECT/CT · Breast cancer

Introduction

The sentinel lymph node (SN) is defined as the first lymph node to which cancer cells are most likely to spread from the primary tumor. The SN biopsy (SNB) technique has been established as a safe and accurate method of screening the axillary nodes for metastasis in the early stage of breast cancer [1]. If the SN is free from cancer, axillary lymph node dissection (ALND) is unnecessary [2, 3]. In addition, many previous studies have demonstrated the same survival results for patients who have undergone increasingly limited axillary surgery [2, 4, 5].

Nuclear scanning, such as single-photon emission computed tomography (SPECT) or functional imaging with F-18-fluorodeoxyglucose (FDG)-positron emission tomography (PET), provides usable information for cancer diagnosis and staging, evaluating the treatment response and/or determining the identification and localization of recurrence. Fusion imaging consisting of SPECT/computed tomography (CT) and FDG-PET/CT yields morphological

✉ Yutaka Yamamoto
ys-yama@triton.ocn.ne.jp

1 Department of Breast and Endocrine Surgery, Faculty of Medical Sciences, Graduate School of Medical Sciences, Kumamoto University, 1-1-1 Honjo, Chuo-ku, Kumamoto, Kumamoto 860-8556, Japan

2 Department of Molecular-Targeting Therapy for Breast Cancer, Kumamoto University Hospital, 1-1-1 Honjo, Chuo-ku, Kumamoto, Kumamoto 860-8556, Japan

3 Department of Diagnostic Radiology, Faculty of Medical Sciences, Kumamoto University, 1-1-1 Honjo, Chuo-ku, Kumamoto, Kumamoto 860-8556, Japan

4 Department of Surgical Pathology, Kumamoto University Hospital, 1-1-1 Honjo, Chuo-ku, Kumamoto, Kumamoto 860-8556, Japan

information on CT and functional information on SPECT and PET [6, 7]. Previous studies have reported that SPECT/CT and FDG-PET/CT are useful for predicting the malignant potential and detecting metastatic LNs in some cancers [8–10]. In particular, SPECT/CT is used to detect the sentinel lymph node in cases of breast cancer [1, 11].

Patients exhibit individual differences in drainage patterns, such that sentinel nodes exist at different locations in different breast cancer patients [12] and it is thus sometimes difficult to determine the exact location of SNs using planar lymphoscintigraphy. The combination of a SPECT camera and CT integrates physiologic and anatomic information, a method that was first described by Lerman et al. [13]. These authors reported that SPECT/CT imaging combined with planar lymphoscintigraphy improved the localization of preoperative draining nodes and considered SPECT/CT to be superior in detecting the SNs missed on planar imaging, such as nodes hidden by scattered radiation at the injection site or due to the atypical SN localization of parasternal lesions [11]. SPECT/CT has also been found to enable the precise characterization of the size, depth and anatomical location of the SN [1] and is thus valuable in enabling surgeons to make a more precise incision. There is a distinct advantage of SPECT/CT navigation for SNB under local anesthesia in patients who need a definite diagnosis of the nodal status for selecting neoadjuvant therapy [14].

On the other hand, the rate of a positive nodal status of SNs in clinically node-negative patients has been reported to be around 30 % [15]. Our preliminary study suggested that a more detailed atypical distribution of SNs out of the "pedestal area", which covers almost the same anatomic extent as Level I, suggests an overall positive nodal status as a reflection of the failure of the lymphatic drainage system [16]. Hence, we believe that it is a better goal to determine whether preoperative imaging of SNs can also be used to predict the status of SNs with sufficient accuracy for the surgeon to decide against ALND.

In this study, we aimed to confirm whether the location of SNs detected using SPECT/CT helps to predict the nodal status of SNs compared with other conventional modalities and clinicopathological factors.

Patients and methods

Patients

From October 2004 to March 2011, we enrolled 381 patients with primary operable invasive breast cancer who were clinically node negative and who underwent SNB. Pathological proof of breast cancer was acquired based on histology or cytology. Informed consent was obtained from all patients according to the regulations of our institution. Patients with a subareolar abscess, inflammatory tumor or metastatic breast cancer and those receiving neoadjuvant chemotherapy or endocrine therapy were excluded.

System design

We used a combined SPECT/CT system that incorporates a commercially available, gantry-free SPECT scanner with dual-head detectors (Skylight; ADAC Laboratories, Milpitas, CA) and an 8-row multi-detector row computed tomography (MDCT) scanner (Light Speed Ultra; GE Healthcare, Little Chalfont, UK). The two scanners were juxtaposed so that the CT table bearing the patient could be moved directly into the SPECT scanner before the CT examination.

CT imaging

The patients were scanned during breath-holding under expiration. Non-contrast, helical CT images for attenuation correction of the SPECT images were obtained at 120 kV, 180 mA, 17.5 mm table feed per rotation, 0.7 s gantry rotation time, 1.25 mm collimation and 1.25 mm reconstruction after the SPECT scan. The CT images were reconstructed using a standard reconstruction algorithm with a 50 cm field of view (FOV) to cover both the patient and the table. The reconstructed images were converted into the DICOM format.

Lymphoscintigraphic technique

On the day before surgery, all patients received a ^{99m}Tc-phytate (FUJIFILM RI Pharma Co., Ltd. Tokyo, Japan) injection of approximately 37 MBq = 1 mL subcutaneously around the areola of the nipple. Lymphoscintigraphy was then performed with SPECT dual-head detector imaging one frame every 30 s for 15 min to identify focal areas of accumulation, followed by the acquisition of multiple 5 min static images. In all patients, delayed images were obtained 3 or 4 h after first imaging session. SPECT was performed 3–4 h after the administration of radiotracer in each patient. The SPECT/CT protocol consisted of 45 projections (180° using two opposing heads) using a Skylight scanner with a vertex ultrahigh-resolution parallel-hole (VXUR) collimator. The reconstructed CT images were processed into Digital Imaging and Communications in Medicine (DICOM) data and transferred to a workstation for SPECT processing by Pegasys (ADAC Laboratories). One lumen of a three-way stopcock (inner diameter 4 mm, length 10 mm) containing an aqueous solution of ^{99m}Tc O_4^- and contrast medium was used as an external fiducial marker. These markers were fixed to the common platform

for SPECT and CT imaging to obtain a precise record. The two scans were performed sequentially. The merging of the SPECT images with the CT images was performed manually by aligning the external fiducial markers of the two images on the workstation. Transaxial, coronal and sagittal sections of the SPECT and CT images were manually integrated to obtain the best matching images on a Zio workstation (Amin Co., Ltd., Tokyo, Japan).

SN mapping with SPECT/CT fusion imaging

The location of each SN was recorded according to the classification of regional lymph nodes developed by the Japanese Society of Clinical Oncology. An axillary lymph node was defined by its position along the axillary vein and its branches as follows: brachial node, distant from the pectoral minor muscle along the axillary vein; subscapular node, along the dorsal thoracic vein; pectoral node, along the lateral thoracic vein; central axillary node, located close to the bottom of the axilla and in contact with the intercostobrachial nerves; subpectoral node, located posterior to the pectoral minor muscle; interpectoral node, located along a branch of the thoracoacromial vein between the pectoral minor muscle and the pectoral major muscle; infraclavicular node, located between the pectoral minor muscle and the deltoideus and below the clavicle; parasternal node, located along the internal thoracic vein. Brachial, subscapular, pectoral and central nodes are defined as Level I nodes [17]. Figures 1, 2 and 3 show the SPECT/CT fusion imaging findings.

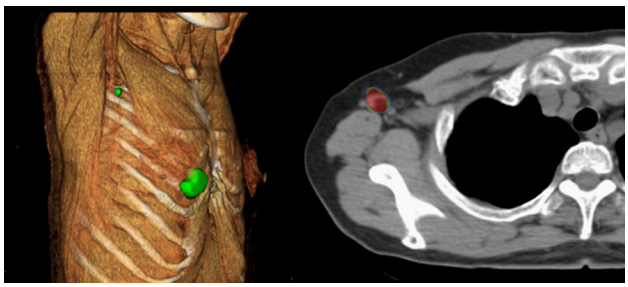

Fig. 1 SPECT/CT fusion imaging in a patient with right breast cancer who exhibited an SN within the Level I (pectoral) area. This is the most common SN location

Surgery

Within 30 h after injection, a handheld gamma probe (neo2000® Gamma Detection System, Mammotome, Cincinnati, OH) was used to identify a hot node. SNs showed a focal uptake of radiotracer up to 10 times the background count rate.

SNs were resected under general anesthesia in patients in whom simultaneous resection of the primary tumor was performed. When resection of the SNs was performed for axillary node staging only, local anesthesia was used. If the SNs were positive, the patient received Level I and II axillary lymph node dissection or neoadjuvant chemotherapy according to the therapeutic protocol of our institution. Supraclavicular and parasternal LN biopsies were not routinely performed.

Pathological examination

In cases of SNB performed simultaneously with primary tumor resection, the SNs were examined intraoperatively as 2 mm frozen sections. After surgery, the SNs were fixed

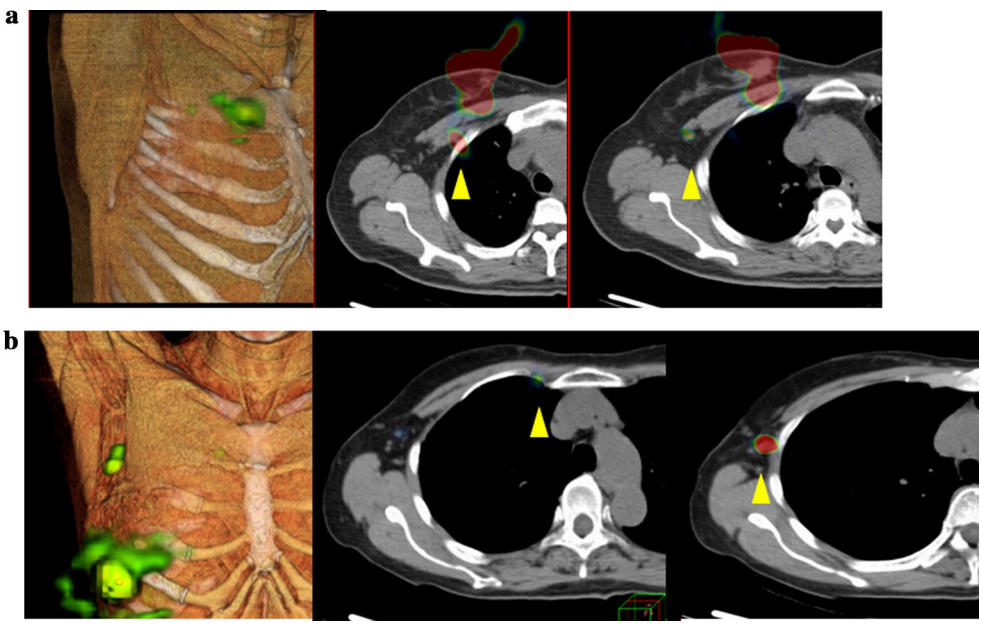

Fig. 2 SPECT/CT fusion imaging in two patients with right breast cancer who demonstrated SNs within Level I and other areas. **a** SPECT/CT imaging of SNs detected in the subpectoral and pectoral areas (*arrowhead*). **b** SPECT/CT imaging of SNs detected in the pectoral and parasternal areas (*arrowhead*)

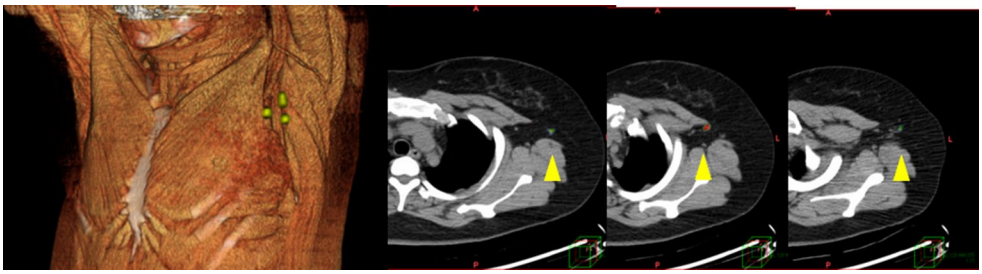

Fig. 3 SPECT/CT fusion imaging in a patient with left breast cancer who showed SNs detected within the Level I area. This case involved three hot nodes in the pectoral area. Actually, at the time of surgery, four SNs were detected using a gamma probe. Two of the four nodes were node positive

in 10 % buffered formalin, processed over 24 h and serially sectioned into ~2 mm slices, which were then embedded in paraffin. The pathological evaluation included routine hematoxylin–eosin staining. SNs removed for axillary staging under local anesthesia were fixed in formalin, sectioned, processed and evaluated according to the same procedure.

Statistical analysis

Statistical comparisons between the groups were carried out using the χ^2 test and logistic regression analysis, and the resulting odds ratio (OR) and 95 % confidence interval (CI) were determined using the JMP statistical software package, Japanese version 10.0.1 (SAS). A P value of <0.05 was considered to be statistically significant.

Results

The characteristics of the patients in this study are listed in Table 1. The median age was 57 years (range 27–81). Two hundred and ninety-eight patients (78.2 %) were node negative and 83 patients (21.7 %) were node positive according to the final histological diagnosis. In one patient (0.26 %), the SN could not be detected using either preoperative SPECT/CT imaging or the intraoperative application of a handheld gamma probe, and SNB was not performed. The results of the additional multivariate analyses of the patient characteristics are shown in Table 2. The rate of node-positive status was lower in older patients ($P = 0.036$). In the multivariate analysis, there was a significant difference between patients <45 years of age and those >65 years of age ($P = 0.0069$, OR: 0.30, CI: 0.09–0.95; Table 2). The extent of tumor invasion was also significantly greater for the node-positive lesions than for the node-negative lesions ($P = 0.0003$; Table 2), between <10 and 10–20 mm lesions (OR: 1.81, CI: 0.72–5.52) and between <10 and >20 mm lesions (OR: 4.35, CI: 1.75–13.2) in the multivariate analysis. The menstrual status, histological type of primary lesion and tumor subtype made no significant contribution to the development of SN metastasis.

The detailed localization of SNs detected using SPECT/CT imaging is indicated in Table 3. The total number of hot nodes was 500, detected in 381 patients. In 355 patients (93.2 %), the nodes were located within the Level I area (94.8 %), while 4.0 % were located in other areas. The SNs in six patients (1.6 %) could not be detected using planar or SPECT/CT imaging. The number of nodes and status of SN metastasis are shown in Tables 4 and 5. We analyzed the relationships for three patterns of SN distribution on SPECT/CT categorized according to the number of nodes and area in which the nodes were located, defined as (a) one node within one area, (b) two nodes within one area and (c) more than three nodes or nothing within one area.

According to univariate analysis of the number of SNs detected on SPECT/CT imaging (a vs b, a vs c, OR: 1.79, 2.83, 95 % CI: 1.03–3.08, 1.29–6.00; $P = 0.011$), the number of SNs detected on SPECT/CT within the Level I area (a vs b, a vs c, OR: 1.80, 3.31, 95 % CI: 1.04–3.11, 1.49–7.18; $P = 0.0048$) or using planar imaging (a vs b, a vs c, OR: 1.87, 2.82, 95 % CI: 1.03–3.08, 1.29–6.01; $P = 0.011$) or with a handheld gamma probe during the operation (a vs b, a vs c, OR: 1.69, 2.83, 95 % CI: 0.98–2.91, 1.35–5.83; $P = 0.012$) and via resection of the SNs (a vs b, a vs c, OR: 1.42, 2.54, 95 % CI: 0.82–2.44, 1.21–5.17; $P = 0.039$) was statistically significant (Tables 4, 5). Among these factors, the contribution of the number of SNs detected on SPECT/CT within the Level I area to the SN status had a higher OR than the other categories. Although we were unable to identify any significant indicators of SN metastasis in the multivariate analysis (Table 5), only the number of SNs detected on SPECT/CT within the Level I area (a vs b, a vs c, OR: 1.55, 3.69, 95 % CI: 0.35–8.12, 0.59–23.5; $P = 0.33$) showed a reasonable OR increment according to the number of SNs detected. Therefore, we performed an additional multivariate analysis of available clinical factors (age and tumor invasion size) and the number of SNs

Table 1 Patient characteristics

	Total ($n = 381$) *n* (%)	Node negative ($n = 298$) *n* (%)	Node positive ($n = 83$) *n* (%)	*P* value
Age				
<45	55 (14.4)	41 (74.6)	14 (25.4)	0.036
45–65	226 (59.3)	170 (75.2)	56 (24.8)	
>65	100 (26.3)	87 (87.0)	13 (13.0)	
Menstrual status				
Premenopause	121 (31.8)	93 (76.9)	28 (23.1)	0.61
Postmenopause	258 (67.7)	203 (78.7)	55 (21.3)	
Male	2 (0.5)	2 (100)	0 (0)	
Tumor invasion size				
<10 mm	36 (13.5)	35 (97.2)	1 (2.8)	<0.0001
10–20 mm	140 (52.4)	119 (85.0)	21 (15.0)	
>20 mm	91 (34.1)	61 (67.0)	30 (33.0)	
Histological type				
IDC	336 (88.2)	260 (77.4)	76 (22.6)	0.37
ILC	13 (3.4)	10 (76.9)	3 (23.1)	
Others	32 (8.4)	27 (87.1)	4 (12.9)	
Subtype				
ER+/Her2−	294 (79.0)	229 (77.9)	65 (22.1)	0.12
Any ER/Her2+	43 (11.6)	30 (69.8)	13 (30.2)	
ER−/Her2−	35 (9.4)	31 (88.6)	4 (11.4)	

IDC invasive ductal carcinoma, *ILC* invasive lobular carcinoma, *ER* estrogen receptor, *Her2* human epidermal growth factor receptor-2

Table 2 Univariate and multivariate analysis of patient characteristics

		Univariate			Multivariate		
		P value	OR	95 % CI	*P* value	OR	95 % CI
Age							
a: <45	a vs b	0.036	0.96	0.49–1.95	0.0069	1.09	0.45–2.86
b: 45–65	a vs c		0.44	0.18–1.01		0.30	0.09–0.95
c: >65							
Menstrual status							
a: Premenopause	a vs b	0.69	0.90	0.54–1.52			
b: Postmenopause							
Tumor invasion size							
a: <10 mm	a vs b	<0.0001	6.17	$1.22–1.12 \times 10^2$	<0.0001	6.85	$1.34–1.25 \times 10^2$
b: 10–20 mm	a vs c		17.20	$3.44–3.12 \times 10^2$		20.90	$4.12–3.83 \times 10^2$
c: >20 mm							
Histological type							
a: IDC	a vs b	0.37	1.02	0.22–3.45			
b: ILC	a vs c		0.48	0.14–1.29			
c: Others							
Subtype							
a: ER +/Her2−	a vs b	0.12	1.52	0.73–3.04			
b: any ER/Her2+	a vs c		2.19	0.83–7.59			
c: ER−/Her2−							

OR odds ratio, *CI* confidence interval

Table 3 Localization of SNs on SPECT/CT imaging

	No.	(%)
Total	500	
Level I area		
Pectoral	435	87
Central	25	5
Subscapular	14	2.8
Other area		
Brachial	1	0.2
Interpectoral	4	0.8
Subpectoral	10	2
Parasternal	5	1
Not detected	6	1.2

detected on SPECT/CT within the Level I area. The results are shown in Table 6. Age (a vs b, a vs c, OR: 1.04, 0.29, 95 % CI: 0.43–2.74, 9.02×10^{-2}–0.94; $P = 0.0089$) and degree of tumor invasion (a vs b, a vs c, OR: 6.77, 21.26, 95 % CI: 1.31–1.24 $\times 10^2$, 4.12–3.91 $\times 10^2$; $P < .0001$) were associated with SN metastasis. Although the number of SNs detected on SPECT/CT within the Level I area was not significantly different (a vs b, a vs c, OR: 1.54, 2.57, 95 % CI: 0.74–3.13, 0.78–7.92; $P = 0.1969$) compared with the clinical factors, it had some visual impact on predicting SN metastasis.

Discussion

The rate of detection of SNs on SPECT/CT has previously been reported to be 84–97.3 %, while our detection rate of 98.8 % was much higher than that of previous reports [15, 18–20]. With regard to SN localization, SNs generally tend to be located at Level I. Data from previous studies have shown that 67.3–96.1 % of SPECT/CT-visualized SNs are located within the Level I area [11, 16, 21]. In our report, the percentage of SNs located within the Level I area was 94.8 %, and only 4.0 % of SNs were located within other areas (brachial, interpectoral, subpectoral and parasternal), while 1.2 % were undetectable. According to the location of hot nodes, 435 SNs (87.0 %) were located within the pectoral area and 20 nodes (4.0 %) within other areas. These data are very similar to those reported in previous studies. In cases in which lymphatic drainage shows an unusual pattern or cannot be seen on planar images, SPECT/CT may be helpful for detecting SNs. Van der Ploeg et al.

Table 4 Number of nodes and status of metastasis

	Total ($n = 381$) n (%)	Node negative ($n = 298$) n (%)	Node positive ($n = 83$) n (%)	P value
Total number of SN detected by SPECT/CT				0.011
1	243 (63.8)	201 (82.7)	42 (17.3)	
2	103 (27.0)	75 (72.8)	28 (27.2)	
≧3 or not detected	35 (9.19)	22 (62.9)	13 (37.1)	
Number of SN detected by SPECT/CT within Level I area				0.0048
1	245 (64.5)	203 (82.9)	42 (17.1)	
2	103 (27.1)	75 (72.8)	28 (27.2)	
≧3 or not detected	32 (8.4)	19 (59.4)	13 (40.6)	
Number of SN detected by SPECT/CT outside Level I area				0.31
1	19 (5.0)	13 (68.4)	6 (31.6)	
2	0 (0)	0 (0)	0 (0)	
≧3 or not detected	362 (95.0)	285 (78.7)	77 (21.3)	
Number of SN detected by planar image				0.011
1	243 (63.8)	201 (82.7)	42 (17.3)	
2	103 (27.0)	75 (72.8)	28 (27.2)	
≧3 or not detected	35 (9.19)	22 (62.9)	13 (37.1)	
Number of SN detected by γ-probe				0.011
1	219 (57.5)	182 (83.1)	37 (16.9)	
2	121 (31.6)	90 (74.4)	31 (25.6)	
≧3 or not detected	41 (10.8)	26 (63.4)	15 (36.6)	
Total number of resected SN				0.039
1	217 (57.0)	178 (82.0)	39 (18.0)	
2	122 (32.0)	93 (76.2)	29 (23.7)	
≧3 or not performed	42 (11.0)	27 (64.3)	15 (35.7)	

Table 5 Univariate and multivariate analyses of the number of nodes and status of SN metastasis

Variables		Univariate			Multivariate		
		P value	OR	95 % CI	*P* value	OR	95 % CI
Number of SN detected by SPECT/CT							
a: 1	a vs b	0.011	1.79	1.03–3.08	0.36	0.91	2.31×10^{-2}–36.86
b: 2	a vs c		2.83	1.29–6.00		1.34	6.31×10^{-4}–2.93×10^{3}
c: ≧3 or not detected							
Number of SN detected by SPECT/CT within Level I area							
a: 1 in Level 1 area	a vs b	0.0048	1.80	1.04–3.11	0.33	1.55	0.35–8.12
b: 2 in Level 1 area	a vs c		3.31	1.49–7.18		3.69	0.59–23.5
c: ≧3 in Level 1 area or not detected							
Number of SN detected by SPECT/CT outside Level I area							
a: 1 in other area	a vs c	0.31	0.58	0.22–1.71			
b: 2 in other area							
c: ≧3 in other area or not detected							
Number of SN detected by planar image							
a: 1	a vs b	0.011	1.87	1.03–3.08	0.99	1.55	2.43×10^{-2}–55.7
b: 2	a vs c		2.82	1.29–6.01		1.33	1.56×10^{-4}–2.42×10^{4}
c: ≧3 or not detected							
Number of SN detected by γ-probe							
a: 1	a vs b	0.012	1.69	0.98–2.91	0.96	4.13	0.64–34.4
b: 2	a vs c		2.83	1.35–5.83		2.33	0.30–18.8
c: ≧3 or not detected							
Total number of resected SN							
a: 1	a vs b	0.039	1.42	0.82–2.44	0.38	3.34	0.60–25.3
b: 2	a vs c		2.54	1.21–5.17		1.28	0.20–8.85
c: ≧3 or not performed							

OR odds ratio, *CI* confidence interval

Table 6 Univariate and multivariate analyses of the patient clinical characteristics and number of SNs detected on SPECT/CT within the Level I area

Variables		Univariate			Multivariate		
		P value	OR	95 % CI	*P* value	OR	95 % CI
Age							
a: <45	a vs b	0.036	0.96	0.49–1.95	0.0089	1.04	0.43–2.74
b: 45–65	a vs c		0.44	0.18–1.01		0.29	9.02×10^{-2}–0.94
c: >65							
Tumor invasion size							
a: <10 mm	a vs b	<0.0001	6.17	$1.22–1.12 \times 10^2$	<0.0001	6.77	$1.31–1.24 \times 10^2$
b: 10–20 mm	a vs c		17.20	$3.44–3.12 \times 10^2$		21.26	$4.12–3.91 \times 10^2$
c: >20 mm							
Number of SN detected by SPECT/CT within Level I area							
a: 1 within Level I area	a vs b	0.0048	1.80	1.04–3.11	0.1969	1.54	0.74–3.13
b: 2 within Level I area	a vs c		3.31	1.49–7.18		2.57	0.78–7.92
c: ≧3 within Level I area or not detected							

[22] found that, among 34 metastatic SNs in 27 patients, four SNs in four patients were detected only on SPECT/CT, whereas the three other nodes in three patients were not detected using lymphoscintigraphy, but were rather identified with blue dye alone. Although there have been no previous reports demonstrating a relationship between the SN location and nodal status, we previously reported that an atypical localization of SNs may suggest axillary positivity as a reflection of the failure of the lymphatic drainage system. We defined the general SN site as the "pedestal area" (PA), that is, the upper part of the pectoral, central and subscapular zones, which form a trapezoidal area. In the node-negative group, 228 lesions (98.3 %) were found in the PA and only four lesions (1.7 %) were outside this area. In contrast, in the node-positive group 65 lesions (78.3 %) were in the PA and 18 lesions (21.7 %) were outside the PA. This difference in SN distribution between the node-positive and node-negative patients was statistically significant ($P < 0.001$) [16].

With regard to the relationship between the number of SNs and the nodal status, Ogasawara et al. [23] reported that an increased number of hot spots visualized using planar lymphoscintigraphy significantly correlates with metastasis. In particular, they showed that metastasis was observed in 57.1 % of patients with more than two visualized nodes, compared to 23.0 % of patients with one node and 22.2 % of patients in whom localization could not be achieved. In our study, metastasis was found in 27.2 % of the patients with two visualized nodes, 17.3 % of the patients with one node and 37.1 % of the patients with more than three nodes or failed localization ($P = 0.011$). Several studies have also suggested that the histological positivity rate for axillary lymph nodes among patients with no SNs detected (including on SPECT/CT) is higher than that noted in patients in whom SNs are detected [1, 16]. Tanis et al. [24] reported that non-visualized SNs identified intraoperatively appear to be tumor positive more often (50 %) than SNs depicted on planar imaging (38 %). In another study, metastatic nodes were identified in 29 % of the patients with clear axillary lymphatic drainage and in 63 % of the patients with no visualized axillary lymphatic drainage [25]. The reason for the identification of negative or scattered SNs on SPECT/CT may be that the existence of metastasis to SNs means that these nodes are occupied by cancer. A sizable metastatic lesion may restrict the inflow of lymphatic fluid and thus radiolabelled colloids. Although only the sensitive technique of SPECT/CT can be used to identify such nodes, alternative nodes become "sentinel" as a result of lymph fluid rerouting and hence acquire a relatively higher radiocolloid uptake. Peritumoral vascular or lymphatic invasion, tumor multifocality and/or distal obstruction of the lymphatics by tumor metastasis can all change the direction of the lymph flow to alternative routes, which may result in an increased number or scattered localization of SNs [26].

Even if SPECT/CT is not successful, it is worthwhile not to stop attempting to detect SNs. Among the six patients in whom no SNs were detected on SPECT/CT in our study, the SNs were successfully detected in four patients using a handheld gamma probe; in two patients, visualization was assisted by blue dye injection. By performing a careful exploration of the axilla with the combined use of blue dye, a gamma probe and intraoperative palpation, a fair number of patients can be identified as node positive and undergo the axillary clearance required, while others can be spared such procedures that do not benefit them [24]. We speculate that our non-withdrawal options for SNB affected the results of the multivariate analysis of the number of resected SN, such that they did not demonstrate inferiority to SPECT/CT (Table 5). Prior to

SNB, the surgeon always simulates the site of incision and the size and depth of the SNs using SPECT/CT. This simulation facilitates the application of a pinpoint biopsy of the SNs. Therefore, using this procedure at the outset to investigate the nodal status assists in determining the therapeutic plan in patients who may need neoadjuvant systemic therapy. Van der Ploeg et al. [22] also reported that SPECT/CT was valuable in facilitating a larger incision in 48 patients (36 %) and an extra incision in six patients (4 %), while incisions were avoided in two patients (1.5 %). Although this assessment of the value of SPECT/CT for facilitating the surgical approach is based on the surgeon's opinion and is therefore somewhat arbitrary, we agree with the authors in a sense as surgeons. Nevertheless, the data should be analyzed more systematically in the future.

The American College of Surgical Oncology Group (ACOSOG) Z0011 trial [27] suggested that there may be no survival benefit in performing ALND in some patients in limited cases, such as those classified as clinical T1 and T2 disease with metastasis only in fewer than three SNs treated with breast-conserving surgery and whole breast irradiation and are eligible for adjuvant systemic therapy. The final analysis of the EORTC 10981-22023 AMAROS (After Mapping of the Axilla: Radiotherapy Or Surgery?) trial demonstrated that both axillary lymph node dissection and axillary radiotherapy provide excellent regional control for breast cancer patients with a positive sentinel node biopsy [28]. It would be beneficial, if possible, to predict whether more than two metastatic nodes are present in the axilla and thus avoid unnecessary ALND. Our data showed that 94.7 % of the patients with only one SN detected on SPECT/CT within the Level I area carried fewer than three metastatic lymph nodes, which suggests that SNB alone may be sufficient for these cases, while the feasibility of axillary irradiation after SNB should be discussed. Therefore, the ability of SPECT/CT to offer accurate detection of SNs as well as predict the particular localization would be extremely valuable.

In conclusion, the detection of anatomical SNs located outside of the Level I area on SPECT/CT raises the possibility that axillary lymph node metastasis can cause obstruction of the lymphatic route or an individual node.

Acknowledgments The authors would like to thank the surgeons, as well as the radiologists, technicians and pathologists, at our institute.

Conflict of interest None to declare.

References

1. Gallowisch HJ, Kraschl P, Igerc I, et al. Sentinel node SPECT-CT in breast cancer. Can we expect any additional and clinically relevant information? Nuklearmedizin. 2007;46:252–6.
2. Krag DN, Anderson SJ, Julian TB, et al. Technical outcomes of sentinel-lymph-node resection and conventional axillary-lymph-node dissection in patients with clinically node-negative breast cancer: results from the NSABP B-32 randomised phase III trial. Lancet Oncol. 2007;8(10):881–8.
3. Nieweg OE, Tanis PJ, Kroon BB. The definition of a sentinel node. Ann Surg Oncol. 2001;8:538–41.
4. Carlson GW, Wood WC. Management of axillary lymph node metastasis in breast cancer: making progress. JAMA. 2011;305(6):606–7.
5. Fisher B, Jeong JH, Anderson S, Bryant J, Fisher ER, Wolmark N. Twenty-five-year follow-up of a randomized trial comparing radical mastectomy, total mastectomy, and total mastectomy followed by irradiation. N Engl J Med. 2002;347(8):567–75.
6. Beyer T, Townsend DW, Brun T, et al. A combined PET/CT scanner for clinical oncology. J Nucl Med. 2000;41(8):1369–79.
7. Schöder H, Yeung HW, Gonen M, et al. Head and neck cancer: clinical usefulness and accuracy of PET/CT image fusion. Radiology. 2004;231(1):65–72.
8. Yoshikawa K, Shimada M, Kurita N, et al. The efficacy of PET-CT for predicting the malignant potential of gastrointestinal stromal tumors. Surg Today. 2013;43(10):1162–7.
9. Karashima R, Watanabe M, Imamura Y, et al. Advantages of FDG-PET/CT over CT alone in the preoperative assessment of lymph node metastasis in patients with esophageal cancer. Surg Today. 2014;45:471–7.
10. Shiraishi S, Tomiguchi S, Utsunomiya D, et al. Quantitative analysis and effect of attenuation correction on lymph node staging of non-small cell lung cancer on SPECT and CT. AJR Am J Roentgenol. 2006;186(5):1450–7.
11. Lerman H, Metser U, Lievshitz G, Sperber F, Shneebaum S, Even-Sapir E. Lymphoscintigraphic sentinel node identification in patients with breast cancer: the role of SPECT-CT. Eur J Nucl Med Mol Imaging. 2006;33:329–37.
12. Estourgie SH, et al. Lymphatic drainage patterns from the breast. Ann Surg. 2004;239:232–7.
13. Keidar Z, Israel O, Krausz Y. SPECT/CT in tumor imaging: technical aspects and clinical applications. Semin Nucl Med. 2003;33:205–18.
14. Iwase H, Yamamoto Y, Kawasoe T, Ibusuki M. Advantage of sentinel lymph node biopsy before neoadjuvant chemotherapy in breast cancer treatment. Surg Today. 2009;39:374–80.
15. Vercellino L, Ohnona J, Groheux D. Role of SPECT/CT in sentinel lymph node detection in patients with breast cancer. Clin Nucl Med. 2014;39:431–6.
16. Ibusuki M, Yamamoto Y, Kawasoe T, et al. Potential advantage of preoperative three-dimentional mapping of sentinel nodes in breast cancer by a hybrid single photon emission CT(SPECT)/CT system. Surg Oncol. 2010;19:88–94.
17. Japanese Society of Clinical Oncology. Classification of regional lymph nodes in Japan. Int J Clin Oncol. 2003;4:248–75.
18. Coffey JP, Hill JC. Breast sentinel node imaging with low-dose SPECT/CT. Nucl Med Commun. 2010;31:107–11.
19. Lerman H, Lievshitz G, Zal O, et al. Improved sentinel node identification by SPECT/CT in overweight patients with breast cancer. J Nucl Med. 2007;48:201–6.
20. Pecking AP, Wartski M, Cluzan RV, et al. SPECT-CT fusion imaging radionuclide lymphoscintigraphy: potential for limb lymphoedema assessment and sentinel node detection in breast cancer. Cancer Treat Res. 2007;135:79–84.
21. Wendler T, Herrmann K, Schnelzer A, et al. First demonstration of 3-D lymphatic mapping in breast cancer using freehand SPECT. Eur J Nucl Med Mol Imaging. 2010;37:1452–61.
22. Van der Ploeg IM, Nieweg OE, Kroon BBR, et al. The yield of SPECT/CT for anatomical lymphatic mapping in patients with breast cancer. Eur J Nucl Med Mol Imaging. 2009;36:903–9.

23. Ogasawara Y, Yoshitomi S, Sato S, Doihara H. Clinical significance of preoperative lymphoscintigraphy for sentinel lymph node biopsy in breast cancer. J Surg Res. 2008;148:191–6.
24. Tanis PJ, van Sandick JW, Nieweg OE, et al. The hidden sentinel node in breast cancer. Eur J Nucl Med Mol Imaging. 2002;29:305–11.
25. Brenot-Rossi I, Houvenaeghel G, Jacquemier J, et al. Nonvisualization of axillary sentinel node during lymphoschintigraphy: is there a pathologic significance in breast cancer? J Nucl Med. 2003;44:1232–7.
26. Sandrucci S, Mussa A, et al. Sentinel lymph node biopsy and axillary staging of T1-T2 N0 Breast cancer: a multicenter study. Semin Surg Oncol. 1998;15:278–83.
27. Giuliano AE, Hunt KK, Ballman KV, et al. Axillary dissection vs no axillary dissection in women with invasive breast cancer and sentinel node metastasis: a randomized clinical trial. JAMA. 2011;305(6):569–75.
28. Journal of Clinical Oncology, In: ASCO Annual Meeting Abstracts. 2013;31, 18_suppl.